NMR Determination of pK_a Values for Asp, Glu, His, and Lys Mutants at Each Variable Contiguous Enzyme−Inhibitor Contact Position of the Turkey Ovomucoid Third Domain[†,‡]

Jikui Song,[§] Michael Laskowski, Jr.,[||] M. A. Qasim,[||] and John L. Markley*[,§]

National Magnetic Resonance Facility at Madison, Department of Biochemistry, University of Wisconsin−Madison, 433 Babcock Drive, Madison, Wisconsin 53706, and Department of Chemistry, Purdue University, West Lafayette, Indiana 47907

Received October 4, 2002; Revised Manuscript Received January 9, 2003

ABSTRACT: From the larger set of 191 variants at all the variable contact positions in the turkey ovomucoid third domain, we selected a subset that consists of Asp, Glu, His, and Lys residues at eight of the nine contiguous $P_6-P_{3'}$ positions (residues 13−21), the exception being P_3-Cys[16] which is involved in a conserved disulfide bridge. Two-dimensional [^{1}H,^{1}H]-TOCSY data were collected for each variant as a function of sample pH. This allowed for the evaluation of 31 of the 32 pK_a values for these residues, the exception being that of P_5-Lys[14], whose signals at high pH could not be resolved from those of other Lys residues in the molecule. Only two of the titrating residues are present in the wild-type protein (P_6-Lys[13] and $P_{1'}$-Glu[19]); hence, these measurements complement earlier measurements by A. D. Robertson and co-workers. This data set was supplemented with results from the pH dependence of NMR spectra of four additional single mutants, P_1-Leu[18]Gly, P_1-Leu[18]Ala, P_2-Thr[17]Val, and $P_{3'}$-Arg[21]Ala, and two double mutants, P_2-Thr[17]Val/$P_{3'}$-Arg[21]Ala and P_8-Tyr[11]Phe/P_6-Lys[13]Asp. Probably the most striking result was observation of a P_2-Thr[17]•••$P_{1'}$-Glu[19] hydrogen bond and a $P_{1'}$-Glu[19]−$P_{3'}$-Arg[21] electrostatic interaction within the triad of P_2, $P_{1'}$, and $P_{3'}$ (residues 17, 19, and 21, respectively). In several cases, the pK_a of a particular residue was sensed by resonances not only in that residue but also in residue(s) with which it interacts. Remarkably, in several interacting systems, resonances from different protons within the same residue yielded different pH_{mid} values.

Proton dissociation constants of individual groups in proteins provide sensitive indicators of intramolecular interactions (*2*−*5*). Residues in disordered regions or in ordered regions with highly exposed side chains are expected to have "normal" pK_a values (*6*). Abnormal pK_a values can indicate the presence of hydrogen bond interactions, electrostatic interactions, or solvent inaccessibility (*7*).

NMR is the most general method for determining pK_a values for individual ionizable groups in small proteins, because signals assigned to individual atoms in nearly all residues usually can be monitored as a function of pH. Changes in chemical shifts with pH report both on specific sites of ionizations (which yield intrinsic pK_a values) and on changes in interactions with surrounding groups resulting from the titration steps. The direction and magnitude of the chemical shift can be indicative of particular interactions. For example, Wüthrich and co-workers (*8*, *9*) have shown that hydrogen bonds between amide protons and carboxylates can be identified on the basis of pH-dependent perturbations of the chemical shifts of the amide protons. When the pH is changed from acidic to neutral across the pK_a of a given acidic group, the resonance from the hydrogen-bonded amide proton shifts to a higher frequency (downfield). In contrast, shifts in the opposite direction result from effects transmitted through covalent bonds; for example, deprotonation of a C-terminal carboxylate or an Asp or Glu side chain results in a shift to a lower frequency (upfield) of the backbone amide proton of that residue (*8*). Studies of polypeptides show that these intrinsic titration shifts in a linear peptide chain typically are smaller than −0.1 ppm for amide protons in nonterminal Asp residues and −0.01 ppm for amide protons in nonterminal Glu residues (*8*).

The turkey ovomucoid third domain, OMTKY3[1] (Figure 1), and bovine pancreatic trypsin inhibitor, BPTI, are the two most and best studied low-molecular weight standard mechanism (*10*), canonical (*11*) protein inhibitors of serine proteinases. As determined from X-ray structures of enzyme−inhibitor complexes, the residues of OMTKY3 marked in black in Figure 1 contact the enzyme and those marked in white do not. Mutations at the black residues generally result in large changes in enzyme−inhibitor equilibrium constants, whereas mutations at the white residues generally have little effect (ref *12* and references therein). The contact residues can be subdivided further into a contiguous set ($P_6-P_{3'}$) and a noncontiguous set ($P_{14'}$, $P_{15'}$, and $P_{18'}$). Within each subset, one residue is clearly structural: P_3-Cys[16] in the contiguous

[†] This work was supported by NIH Grant P41 RR 02301 (to J.L.M.) and Grants GM 10831 and GM 63539 (to M.L.).

[‡] The assigned pH-dependent chemical shifts and the resulting titration parameters have been deposited (as 43 separate files, bmrb entries 5411−5453) at BioMagResBank.

* To whom correspondence should be addressed. Phone: (608) 263-9349. Fax: (608) 262-3759. E-mail: markley@nmrfam.wisc.edu.

[§] University of Wisconsin−Madison.

[||] Purdue University.

10.1021/bi0269512 CCC: $25.00
Published on Web 02/20/2003

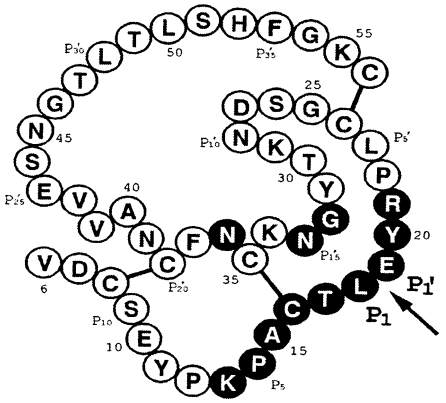

FIGURE 1: Amino acid sequence of the turkey ovomucoid third domain (OMTKY3) (*41*). The 12 consensus proteinase contact residues (*42*) are highlighted in black. The reactive site peptide bond between the P_1 residue (Leu[18]) and the $P_{1'}$ residue (Glu[19]) is denoted with an arrow.

set and $P_{15'}$-Asn[33] in the noncontiguous set. In this paper, we concentrate on only the eight nonstructural residues of the contiguous set.

We earlier had substituted each of the 10 nonstructural contiguous and noncontiguous contact residues with each of the 19 other standard amino acids and determined the equilibrium constants (and therefore standard free energies of association) for the association of these 191 variants with six selected enzymes (*12*). Assuming that the standard free energies of association at all 10 positions are additive, one can calculate the standard free energy of association of any Kazal family inhibitor with one of these six selected enzymes. Such predictions for the 500 known equilibrium constants for natural, synthetic, and semisynthetic Kazal inhibitor variants showed them to be at least partially addititive in ~90% of the cases (ref *12* and unpublished studies). However, this simple additivity scheme works only at the pH value (in our case pH 8.30) where the equilibrium constants were determined. Because different biological systems employ different pH values, predictions over a broad pH range clearly would be useful.

For many of the black residues in Figure 1, complex formation involves a transfer of the residue, which is largely exposed to solvent in the free inhibitor, to the hydrophobic interior of a cavity in the enzyme. This is particularly clear for transfer of the P_1 residue from its "hyperexposed" state in the free inhibitor to the hydrophobic S_1 pockets of chymotrypsin, elastases, SGPA, or SGPB. Qasim et al. (*13*) showed that such environmental transfer in SGPB changes the pK_f (the pK_a in the free form of the inhibitor) of P_1-Asp[18] from 4.40 to 9.26. This huge shift in pK_f greatly affects the pH dependence of the association equilibrium constant. However, additivity can still be employed, provided that both the $\Delta G°_{TKY}$ and $\Delta\Delta G°(X_{TKY}i\ X)$ terms are not just constants but pH-dependent functions. Such functions are given by (*14*)

$$\Delta\Delta G°(X_{TKY}i\ X)(pH) = \Delta\Delta G°(X_{TKY}i\ X\ \text{protonated}) + RT\ln\frac{1+10^{-(pH-pK_c)}}{1+10^{-(pH-pK_f)}} \quad (1)$$

It seemed to us at first that the three parameters of this equation could be readily determined by measuring the pH dependence of $\Delta G°$. This proved to be quite wrong as $\Delta G°$(pH) becomes very difficult to measure below pH 4 and above pH 10. Values of pK_f are expected to lie outside this region, certainly for Lys, and probably also for Asp and Glu, thus precluding accurate determination of pK_f from K_a data.

Access to independent measurements of pK_f values for residues in the contact region would increase the accuracy of the predicted values of association constants. This was the rationale for the present NMR determination of such values. For completeness, His was included along with Asp, Glu, and Lys discussed above. These four residues were placed at each of the eight contiguous, variable contact positions. OMTKY3 naturally has P_6-Lys[13] and $P_{1'}$-Glu[19]. Therefore, the target set included 31 OMTKY3 variants: wild-type OMTKY3 and 30 ($4 \times 8 = 32 - 2 = 30$) single mutants. We have been able to measure pK_f values for all but P_5-Lys[14], which proved to be intractable because its side chain signals could not be distinguished from those of the other four Lys side chains of the variant. The database of these pK_f values will be of great aid in analyzing data on complex formation. A limited but interesting application of this type has been published (*14*) in which the pH behavior of a P_1 lysyl side chain was compared [in a substrate molecule, in BPTI (which has a natural P_1-Lys), and in P_1-Leu[18]Lys OMTKY3] both by the pH dependence of K_{assoc} and by X-ray crystallographic comparison of complexes with a protonated lysyl side chain at P_1.

A particularly valuable aspect of determining titration behavior of free inhibitors is that the magnitude of pK_f in eq 1 depends only on the inhibitor while the value of pK_c depends on both the inhibitor and the enzyme. Thus, one pK_f value serves the studies of that particular residue at a specified position in complexes with all possible serine proteinases. Because the variable contact positions are all relatively exposed, it is not surprising that most of the pK_f values were found to be similar to unperturbed values. However, a few exhibited larger differences, and these were subjected to additional investigation. For example, interactions within the P_2-Thr[17], $P_{1'}$-Glu[19], $P_{3'}$-Arg[21] triad were analyzed by reference to pH titration studies of two additional single mutants, P_2-Thr[17]Val and $P_{3'}$-Arg[21]Ala, and one double mutant, P_2-Thr[17]Val/$P_{3'}$-Arg[21]Ala.

[1] OMTKY3 stands for the third domain of the proteinase inhibitor (ovomucoid) from turkey (*Meleagris gallopavo*) (Swiss-Prot entry P01004). Residues in OMTKY3 are denoted as P_i-Xxx^j, where P denotes the Schecter−Berger notation for proteinase inhibitors (*1*) with i values for residues to the N-terminal side of the cleavage site and i' values for those to the C-terminal side, Xxx is the three-letter amino acid code, and j is the residue number according to the 56-residue OMTKY3 domain (that starting with the sequence L[1]AAVS[5]...). OMTKY3 mutants are described by a dual notation, e.g., $P_{5'}$-Pro[14]Asp for substitution of $P_{5'}$-Pro[14] with Asp. Note that in this study all single mutant forms of OMTKY3 were in the 51-residue background starting at Val[6] and both double mutant forms were in the 56-residue background starting at Leu[1]. Titration shifts $\Delta\delta$ are reported as the proton chemical shift at the high-pH plateau minus that at the low-pH plateau: $\Delta\delta = \delta_{A^-} - \delta_{HA}$. Inflection points derived from NMR pH titration curves (pH dependence of chemical shifts) are designated as pH_{mid} values. If a pH_{mid} value can be associated with a particular deprotonation step, it is designated as a pK_a value. The notation pK_f denotes a pK_a of a group in the free inhibitor, and pK_c denotes a pK_a of a group in an inhibitor−proteinase complex. Chemical shifts to higher frequencies (downfield) are positive; chemical shifts to lower frequencies (upfield) are negative. Abbreviations: [^{1}H,^{1}H]-TOCSY, two-dimensional homonuclear total correlation spectroscopy; OMSVP3, third domain from silver pheasant ovomucoid; TPPI, time-proportional phase incrementation; SNase, staphylococcal nuclease; WT, wild-type.

Wild-type OMTKY3 undergoes cis ↔ trans isomerism of the P_8-Tyr^{11}−P_7-Pro^{12} peptide bond at very low pH (*15*), and some of the mutants employed here exhibited this transition at altered pH_{mid} values. We have determined the structural consequences, kinetics, and thermodynamics of this interesting transition as a further step in our understanding of pH-dependent processes in OMTKY3 and its contact region variants; these results will be presented separately (J. Song, M. Qasim, M. Laskowski, Jr., and J. L. Markley, manuscript in preparation).

EXPERIMENTAL PROCEDURES

Expression and Purification of OMTKY3 Variants. Published methods were employed in preparing the OMTKY3 variants with single-residue substitutions (*16*, *17*). These variants, which lacked residues 1−5 of the full-length OMTKY3 sequence, contained 51 residues (6−56).

Two double-mutant forms of OMTKY3 (P_2-Thr^{17}Val/$P_{3'}$-Arg^{21}Ala and P_8-Tyr^{11}Phe/P_6-Lys^{13}Asp) were prepared by a slight modification of a published procedure (*18*). Full-length OMTKY3 (containing residues 1−56) was produced as an N-terminal fusion with staphylococcal nuclease; the fusion protein contained an engineered cyanogen bromide cleavage site in the linker between the two proteins (*18*). The gene encoding SNase was modified so that all Met residues were changed to Ala (to eliminate additional cyanogen bromide cleavage sites), and the fusion protein was purified from inclusion bodies isolated from the harvested BL-21 cells used for protein expression (*19*). GdmCl (6 M) and DTT (100 mM) were added to denature the fusion protein; these reagents were removed later by dialysis against 0.1 M acetic acid. Protein renaturation was achieved by fast dilution into 50 mM Tris buffer (pH 8.0) containing 1.74 mM β-mercaptoethanol. The fusion protein was removed by CNBr cleavage at pH 1.0, and the desired product was purified by reversed-phase HPLC.

NMR Sample Preparation. Samples used for NMR data collection contained 2−3 mM OMTKY3 variant dissolved in a 90% H_2O/10% D_2O mixture (v/v) containing 100 mM potassium chloride and 0.4 mM 2,2-dimethylsilapentane-5-sulfonic acid (DSS). The pH of the solution was adjusted by adding aliquots of concentrated HCl or KOH. The pH of the sample at room temperature was measured both before and after the NMR data were collected, and the average reading was used for data analysis. The difference between these readings generally was <0.05 pH unit. The glass electrode (Biological Combination Electrode, Beckman, Fullerton, CA) was calibrated with commercial standard pH buffers 1.0, 4.0, 7.0, 10.0, and 11.0 (Fisher Scientific, Fair Lawn, NJ). A degassed saturated solution of $Ca(OH)_2$ at 25 °C served as the pH 12.42 standard (*20*). Two buffers spanning the pH of interest were used in calibrating the electrode.

NMR Experiments and Data Processing. Two-dimensional (2D) [^{1}H,^{1}H]-TOCSY (total correlated spectroscopy) data with time-proportional phase incrementation were collected on Bruker DMX500 and DMX600 spectrometers located in the National Magnetic Resonance Facility at Madison. A Watergate 3-9-19 pulse sequence (*21*) was used for solvent suppression. In all experiments, the carrier frequency was set at the middle of the spectrum, and the mixing times were 50 ms. All NMR data were collected at a probe temperature of 25 °C calibrated by a methanol NMR standard. All NMR spectra were processed using XWINNMR software (Bruker, Billerica, MA) installed on Silicon Graphics (Mountain View, CA) workstations.

Data Fitting. Titration data can be fitted to simple models that assume no interaction with neighboring groups or to more complex models that take various kinds of interactions into account, but require the fitting of additional parameters. The simple model can be extended to account for remote interactions by introducing the Hill coefficient as an additional parameter (*22*). Titration data from monophasic transitions were fitted to eq 2 with a software package written by H. W. Anthonsen (available from www.nmrfam.wisc.edu/~hwa).

$$\delta_{obs} = \delta_B + \frac{\Delta\delta \times 10^{n(pK_a - pH)}}{1 + 10^{n(pK_a - pH)}} \quad (2)$$

Biphasic titration data were fitted to eq 3 by the nonlinear least-squares analysis using Sigma Plot (Microsoft Package).

$$\delta_{obs} = \delta_B + \frac{\Delta\delta_1 \times 10^{n_1(pK_{a1} - pH)}}{1 + 10^{n_1(pK_{a1} - pH)}} + \frac{\Delta\delta_2 \times 10^{n_2(pK^{a2} - pH)}}{1 + 10^{n_2(pK^{a2} - pH)}} \quad (3)$$

In eqs 2 and 3, δ_{obs} and δ_B represent the observed peak chemical shift at a particular pH and the chemical shift of the unprotonated form, respectively. $\Delta\delta$, $\Delta\delta_1$, and $\Delta\delta_2$ represent titration shifts; n, n_1, and n_2 are Hill coefficients (*22*).

RESULTS AND DISCUSSION

Complications in Data Analysis

Multiple pH-Dependent Influences on Chemical Shifts. The Hill coefficient n, defined in eq 4, where Y is the fraction of ionization of the group of interest, provides a first-order approach to dealing with interactions between sites with similar pK_a values.

$$Y = \frac{(K_a/[H^+])^n}{1 + (K_a/[H^+])^n} \quad (4)$$

The pH-dependent chemical shift data from a single non-interacting proton dissociation site, such as that in a monoprotic acid, are expected to fit a simple titration curve (eq 2 with $n = 1$). In a molecule containing two or more proton dissociation sites with similar pK_a values, the addition of a proton at adjacent site(s) has the electrostatic effect of lowering the pK_a of the site being examined. This flattens out the titration curve and yields a Hill coefficient of <1 (eq 2 with $n < 1$; negative cooperativity). Most n values reported here are <1, as expected. Proteins are complex enough to occasionally exhibit positively cooperative ionizations. If the protonation of a remote site increases the pK_a of the examined site, this has the effect of making the titration curve steeper and yields a Hill coefficient of >1 (eq 2 with $n > 1$).

The observation of a pH-dependent shift in an NMR signal from a given residue does not necessarily indicate that the

Table 1: ^{1}H NMR Chemical Shifts, pH_{mid} Values, and Hill Coefficients for P_2-Asp^{17} and $P_{3'}$-Asp^{21} in Their Respective OMTKY3 Variants[a]

	NMR signal followed[b]	δ_{A^-} (ppm)	$\Delta\delta$ (ppm)[c]	pH_{mid}	Hill coefficient
P_2-Asp^{17} (in P_2-Thr^{17}Asp)	$^1H^{\beta}$	2.75	−0.29	3.44 (0.03)	0.83 (0.04)
	$^1H^{\beta'}$	2.94	−0.27	4.14 (0.05)	0.82 (0.08)
	$^1H^N$	8.49	−0.20	3.70 (0.04)	0.72 (0.04)
$P_{3'}$-Asp^{21} (in $P_{3'}$-Arg^{21}Asp)	$^1H^{\beta}$	2.47	−0.29	4.00 (0.04)	0.92 (0.07)
	$^1H^{\beta'}$	2.72	−0.16	3.57 (0.04)	0.94 (0.06)

[a] The numbers in parentheses are standard deviations returned by the software fitting the titration curves. [b] The signals from the two geminal protons of aspartate ($^1H^{\beta 2}$ and $H^{\beta 3}$) were not chirally assigned; that with the smaller δ_{A^-} value is designated $^1H^{\beta}$ and that with the larger δ_{A^-} value $^1H^{\beta'}$. [c] $\Delta\delta = \delta_{A^-} - \delta_{HA}$.

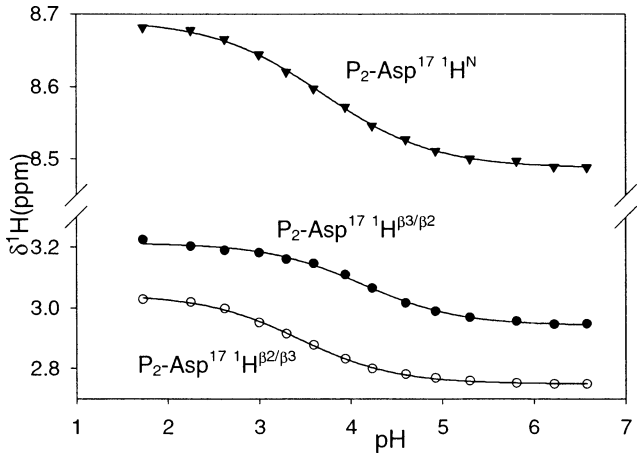

FIGURE 2: pH dependence of the chemical shifts of P_2-Asp^{171} H^N, $^1H^{\beta 2}$, and $^1H^{\beta 3}$ in P_2-Thr^{17}Asp OMTKY3. The methylene protons were not assigned stereospecifically. The curves represent the best fits to the data points.

protonation step is occurring in that residue. The assignment of the pH-dependent shift to a particular protonation site has to be made on the basis of additional information, such as which nuclei are affected and the directions and magnitudes of their titration shifts.

If the site being examined is influenced by two protonation steps with pK_a values that differ by more than 1 pH unit, then two pH-dependent inflections may be resolved, which can be fitted to eq 3. The shape of the curve will depend on the direction of the titration shift for each step. One of the inflections may reflect the protonation of the residue whose chemical shift is examined with the other representing a remote ("spectroscopic") interaction. Alternatively, both may be remote.

It is important to unravel individual influences on chemical shifts when signals from a particular residue show multiple pH effects. One such example is P_2-Asp^{17} in the mutant P_2-Thr^{17}Asp (Figure 2). The pH_{mid} values obtained from the pH dependence of the chemical shifts of the two prochiral $^1H^{\beta}$s were 3.44 and 4.13, whereas that from $^1H^N$ was 3.7 with a titration shift of −0.2 ppm (Table 1). The value of 4.13 is probably closer to the "microscopic" pK_a of P_2-Asp^{17} than the other two values, considering the spatial proximity between P_2-Asp^{17} and $P_{1'}$-Glu^{19}. All three Hill coefficients returned by fitting the data from the $^1H^N$, $^1H^{\beta 2}$, and $^1H^{\beta 3}$ chemical shifts of P_2-Asp^{17} were significantly <1, consistent with an electrostatic interaction with the neighboring $P_{1'}$-Glu^{19}. A similar effect was seen in the mutant $P_{3'}$-Arg^{21}Asp, where the pH_{mid} values determined from the two $^1H^{\beta}$s of $P_{3'}$-Arg^{21} differed by 0.43 pH unit, also likely from electrostatic interaction with $P_{1'}$-Glu^{19}. In mutant P_2-Thr^{17}Asp, $^1H^N$ of $P_{1'}$-Glu^{19} yielded a pH_{mid} of 3.52 and a titration shift of 0.29 ppm. The actual pK_a of $P_{1'}$-Glu^{19} in this mutant may be higher than this apparent value. Chemical shielding from the negatively charged P_2-Asp^{17} appears to counteract the deshielding effect of the hydrogen bond on the $P_{1'}$-Glu^{19} $^1H^N$ chemical shift. This interaction is reflected in the value of the Hill coefficient (0.70) for the titration curve of $P_{1'}$-Glu^{19}, which suggests that the effect involves more than protonation at the single site. This conclusion is consistent with mutual electrostatic interaction between the P_2 and $P_{1'}$ sites in P_2-Thr^{17}Asp, which as described below was deduced from the pH dependence of signals from P_2-Thr^{17}. As noted below, introduction of a longer carboxylate side chain at P_2 (P_2-Thr^{17}Glu) abolishes the $P_2-P_{1'}$ interaction.

Conformational Equilibrium at Low pH. OMTKY3 variants with P_5-(Asp^{14}/Glu^{14}/His^{14}) or P_6-(Asp^{13}/Glu^{13}) exhibited pH-dependent structural heterogeneity, as evidenced by the presence for various residues of two sets of NMR peaks with pH-dependent relative intensities. Similar peak doubling was seen in spectra of P_1-Gly^{18} OMTKY3. The origin of this conformational heterogeneity, its effects on pK_a values, and the three-dimensional structures of the two interconverting states will be presented separately (J. Song, M. A. Qasim, M. Laskowski, Jr., and J. L. Markley, manuscript in preparation). The report presented here concerns only the conformational state that predominates at neutral pH.

Titration Results for the Substituted Sites

From NMR titration studies of the 32 OMTKY3 variants, pK_a values were determined for each of four different titratable residues (Asp, Glu, His, and Lys) at each of eight residue positions (residues $P_6-P_{3'}$ with the exception of P_3-Cys^{16}). Full titration results are listed in Table 2. Although pK_a values for P_6-Lys^{13} and $P_{1'}$-Glu^{19} in wild-type OMTKY3 have been reported (*23*, *24*), they were remeasured under the experimental conditions of the current study. Signals from the lysines inserted into the proteinase binding loop were found to overlap with those of $P_{16'}$-Lys^{34} and $P_{37'}$-Lys^{55}. The uniformity of the chemical shifts (near-random coil values) of the lysine side chains suggests that these residues are all solvent-exposed and flexible. The pK_a of the lysine introduced into the P_5-Pro^{14} position was not determined, because NMR peaks from this residue could not be resolved in [^{1}H,^{1}H]-TOCSY spectra. A full titration curve was determined for P_6-Lys^{13} present in wild-type OMTKY3, but the high-pH end points were not reached for the lysines at other positions; this degraded the accuracy of their pK_a determinations.

Titratable Groups at the P_6 Position (Residue 13). The pK_a value of P_6-Lys^{13} in wild-type OMTKY3 determined

Table 2: ^{1}H NMR Chemical Shifts, Measured pK_a Values, and Hill Coefficients of Titratable Residues in Various OMTKY3 Variants with Single-Site Replacements along with Data for Model Peptides[a]

residue	amino acid[b]	NMR signal followed	δ_{A^-} (ppm)	$\Delta\delta$ (ppm)[c]	pK_a	Hill coefficient	variation from model pK_a values[d]
P_6-Lys^{13}	Asp[e]	$^1H^{\beta2/\beta3}$	2.29	−0.32	4.33 (0.03)	0.84 (0.04)	0.49
	Glu	$^1H^N$	9.38	0.05	5.48 (0.09)	1.69 (0.40)	1.16
	His	$^1H^{\epsilon1}$	7.54	−0.93	6.73 (0.01)	0.96 (0.02)	0.23
	Lys	$^1H^{\epsilon2/\epsilon3}$	1.99	−0.56	9.65 (0.05)	0.80 (0.07)	−0.85
P_5-Pro^{14}	Asp	$^1H^{\beta2/\beta3}$	2.66	−0.25	3.82 (0.03)	0.97 (0.05)	−0.02
	Glu	$^1H^{\gamma2/\gamma3}$	2.29	−0.23	4.39 (0.03)	0.95 (0.06)	0.07
	His	$^1H^{\epsilon1}$	7.68	−0.96	6.38 (0.02)	1.02 (0.03)	−0.12
P_4-Ala^{15}	Asp	$^1H^{\beta2/\beta3}$	2.59	−0.30	3.95 (0.02)	1.06 (0.05)	0.11
	Glu	$^1H^{\gamma2/\gamma3}$	2.14	−0.25	4.32 (0.04)	0.93 (0.07)	0.00
	His	$^1H^{\epsilon1}$	7.64	−0.99	6.49 (0.01)	0.98 (0.01)	−0.01
	Lys	$^1H^{\epsilon2/\epsilon3}$	2.57	−0.42	10.43 (0.01)	0.93 (0.02)	−0.07
P_2-Thr^{17}	Asp[f]	$^1H^{\beta2/\beta3}$	2.94	−0.27	4.14 (0.05)	0.82 (0.08)	0.30
	Glu	$^1H^N$	9.62	0.92	3.91 (0.02)	0.95 (0.03)	−0.41
	His	$^1H^{\epsilon1}$	7.69	−0.95	5.98 (0.02)	0.89 (0.03)	−0.52
	Lys	$^1H^{\epsilon2/\epsilon3}$	2.61	−0.41	10.40 (0.04)	0.89 (0.07)	−0.10
P_1-Leu^{18}	Asp	$^1H^{\beta2/\beta3}$	2.77	−0.25	3.87 (0.04)	0.81 (0.05)	0.03
	Glu	$^1H^{\gamma2/\gamma3}$	2.30	−0.26	4.19 (0.04)	0.97 (0.07)	−0.13
	His	$^1H^{\epsilon1}$	7.71	−0.94	6.51 (0.02)	0.89 (0.03)	0.01
	Lys	$^1H^{\epsilon2/\epsilon3}$	2.65	−0.39	10.70 (0.03)	1.06 (0.07)	0.20
$P_{1'}$-Glu^{19}	Asp	$^1H^{\beta2/\beta3}$	2.53	−0.32	3.13 (0.03)	0.92 (0.05)	−0.71
	Glu	$^1H^N$	8.23	0.60	3.54 (0.02)	1.04 (0.03)	−0.78
	His	$^1H^{\epsilon1}$	7.76	−0.97	5.68 (0.01)	0.99 (0.02)	−0.82
	Lys	$^1H^{\epsilon2/\epsilon3}$	2.59	−0.44	10.10 (0.12)	0.74 (0.13)	−0.40
$P_{2'}$-Tyr^{20}	Asp	$^1H^{\beta2/\beta3}$	2.59	−0.28	3.90 (0.04)	1.0 (0.08)	0.06
	Glu	$^1H^{\gamma2/\gamma3}$	2.37	−0.16	4.29 (0.05)	0.73 (0.07)	−0.03
	His	$^1H^{\epsilon1}$	7.65	−1.06	6.00 (0.01)	0.98 (0.02)	−0.50
	Lys	$^1H^{\epsilon2/\epsilon3}$	2.63	−0.42	10.40 (0.03)	0.90 (0.06)	−0.10
$P_{3'}$-Arg^{21}	Asp[f]	$^1H^{\beta2/\beta3}$	2.47	−0.29	4.00 (0.04)	0.92 (0.07)	0.16
	Glu	$^1H^{\gamma2/\gamma3}$	2.11	−0.27	4.56 (0.05)	0.87 (0.09)	0.24
	His	$^1H^{\epsilon1}$	7.62	−1.01	6.72 (0.01)	0.92 (0.01)	0.22
	Lys	$^1H^{\epsilon2/\epsilon3}$	2.54	−0.43	10.72 (0.02)	0.93 (0.03)	0.22
model compounds							
Suc-AAPX-pna							
X = Asp		$^1H^{\beta2/\beta3}$	2.78	−0.29	3.84 (0.02)	0.91 (0.04)	
X = Glu		$^1H^{\gamma2/\gamma3}$	2.34	−0.24	4.32 (0.02)	1.05 (0.04)	
X = Lys		$^1H^{\epsilon2/\epsilon3}$	2.61	−0.43	10.51 (0.02)	0.95 (0.02)	
H-GGXA-OH[g]							
X = Asp					3.9 (0.1)		
X = Glu					4.3 (0.01)		
X = His					7.0 (0.1)		
X = Lys					11.1 (0.2)		

[a] The numbers in parentheses are standard deviations returned by the software fitting the titration curves. [b] The wild-type residues at positions P_6 and $P_{1'}$ are bold. [c] $\Delta\delta = \delta_{A^-} - \delta_{HA}$. [d] Standard p$K_a$ values assumed here were 3.84 for Asp, 4.32 for Glu, 6.50 for His, and 10.5 for Lys; see the text. [e] The pH titration parameters for P_6-Asp^{13} were determined from the double mutant P_8-Tyr^{11}Phe/P_6-Lys^{13}Asp. [f] The pH dependence of the chemical shifts of $^1H^{\beta2}$ and $^1H^{\beta3}$ nuclei exhibited different inflections. On the basis of charge−charge interactions, it was deduced that the inflection yielding the higher pH_{mid} represents the pK_a value. [g] From Bundi and Wüthrich (*6*).

here (9.65 ± 0.05) is similar to the value reported previously (9.86) (*23*). Surprisingly, neither $^1H^{\beta2/\beta3}$ of P_6-Asp^{13} nor $^1H^{\gamma2/\gamma3}$ of P_6-Glu^{13} exhibited an observable pH dependence. The pK_a value for Glu inserted at the P_6 position of OMTKY3 was determined from the pH dependence of its $^1H^N$ signal. The pH titration data for P_6-Asp^{13} were determined in the double mutant (P_8-Tyr^{11}Phe/P_6-Lys^{13}Asp), which exhibited an observable titration shift for one of the $^1H^{\beta}$ protons (Table 1). These findings suggest that a ring current effect from P_8-Tyr^{11} could be responsible for masking the expected pH dependence of these signals. Robertson et al. (*25*) proposed such a ring-current mechanism to explain the failure of one $^1H^{\epsilon}$ of P_6-Lys^{13} in wild-type OMTKY3 to exhibit an appreciable titration shift.

Site Specific pK_a Perturbations. Reference values for unperturbed chemical shifts and pK_a values were reported by Bundi and Wüthrich (*6*) for the H-Gly-Gly-Xxx-Ala-OH tetrapeptides (reproduced in Table 1): 3.9 ± 0.1 for Asp, 4.3 ± 0.1 for Glu, 7.0 ± 0.1 for His, and 11.1 ± 0.2 for Lys. Additional data were determined here for the Suc-Ala-Ala-Pro-Xxx-pna model peptide: 3.84 ± 0.02 for Asp, 4.32 ± 0.02 for Glu, and 10.51 ± 0.02 for Lys (Table 1). These are comparable to the values of Bundi and Wüthrich, except for the value for Lys, which is somewhat lower. A pK_a of 6−7 has been reported for the imidazole of histidine in a denatured protein (*6*, *26*−*28*). Standard pK_a values assumed here were as follows: 3.84 for Asp, 4.32 for Glu, 6.50 for His, and 10.5 for Lys.

Differences between the observed pK_a values and these standard values are shown in the right-most column of Table 2. The results show that context-dependent perturbations are smallest at P_5 and P_1 and largest at P_6 and $P_{1'}$. By residue type, the patterns are highly site specific: the pK_a values of Asp and Glu are both higher than normal when at P_6 and both lower than normal at $P_{1'}$. Lys shows a large perturbation at only P_6. The pK_a of His is depressed significantly when located at P_2, $P_{1'}$, or $P_{2'}$.

Table 3: Fitted ^{1}H NMR Chemical Shifts, Measured pK_a Values, and Hill Coefficients of $P_{1'}$-Glu^{19} in Various OMTKY3 Variants[a]

OMTKY3 variant	proton of $P_{1'}$-Glu^{19} observed	δ_{A^-} (ppm)	$\Delta\delta$[b] (ppm)	pK_a (error)	Hill coefficient (error)	pK_a change from the WT value (error)
wild type	$^1H^N$	8.23	0.60	3.54 (0.02)	1.04 (0.03)	
P_6-Lys^{13}Glu	$^1H^N$	8.12	0.46	3.47 (0.02)	1.08 (0.04)	−0.07 (0.04)
P_5-Pro^{14}Glu	$^1H^N$	8.22	0.55	3.58 (0.01)	0.96 (0.02)	0.04 (0.03)
P_4-Ala^{15}Glu	$^1H^N$	8.17	0.47	3.49 (0.01)	1.06 (0.03)	−0.05 (0.03)
P_2-Thr^{17}His	$^1H^N$	8.20	0.21	3.55 (0.03)	1.10 (0.07)	0.01 (0.05)
P_2-Thr^{17}Val	$^1H^N$	7.89	0.17	3.92 (0.03)	1.10 (0.07)	0.38 (0.05)
	$^1H^{\gamma2/\gamma3}$	2.21	0.25	3.92 (0.04)	0.91 (0.06)	0.38 (0.06)
P_2-Thr^{17}Val/$P_{3'}$-Arg^{21}Ala	$^1H^{\gamma2/\gamma3}$	2.22	0.23	4.11 (0.02)	0.91 (0.04)	0.57 (0.04)
P_1-Leu^{18}Asp	$^1H^N$	8.11	0.47	3.21 (0.02)	1.34 (0.06)	−0.33 (0.03)
P_1-Leu^{18}Glu	$^1H^N$	8.22	0.54	3.39 (0.01)	1.10 (0.01)	−0.15 (0.03)
$P_{2'}$-Tyr^{20}Asp	$^1H^N$	8.05	0.32	3.98 (0.04)	1.36 (0.15)	0.44 (0.06)
$P_{2'}$-Tyr^{20}Glu	$^1H^N$	8.13	0.43	3.86 (0.02)	1.00 (0.04)	0.32 (0.04)
$P_{3'}$-Arg^{21}Asp	$^1H^N$	8.48	0.86	3.91 (0.02)	0.87 (0.04)	0.37 (0.04)
$P_{3'}$-Arg^{21}Glu	$^1H^N$	8.89	1.28	3.91 (0.02)	0.77 (0.03)	0.37 (0.04)
$P_{3'}$-Arg^{21}Ala	$^1H^N$	8.37	0.74	3.77 (0.02)	0.97 (0.03)	0.23 (0.04)

[a] The numbers in parentheses are standard deviations returned by the software fitting the titration curves. [b] $\Delta\delta = \delta_{A^-} - \delta_{HA}$.

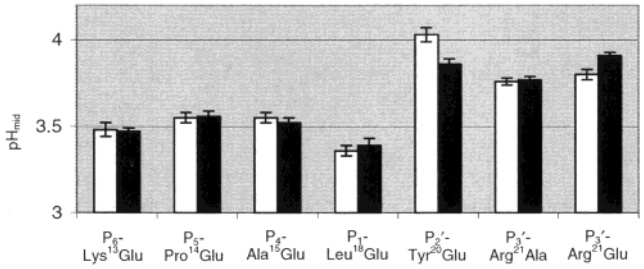

FIGURE 3: Comparison of pH$_{mid}$ values for the titration shifts of P_2-Thr^{171} H^N (white bars) and $P_{1'}$-Glu^{191} H^N (black bars) in different OMTKY3 variants.

Effects of Substitutions on Other Titrations in OMTKY3

In addition to the pK_a values of the residues introduced into the contact region of OMTKY3 (Table 2), the NMR titration data include perturbations of other pK_a values resulting from the substitutions. Such results provide information about longer-range molecular interactions within the molecule.

$P_{1'}$-Glu^{19}. An interesting case is the side chain carboxyl group of $P_{1'}$-Glu^{19}, which is responsive to mutations at several other residue positions (Table 3). The pK_a value of $P_{1'}$-Glu^{19} in wild-type OMTKY3 determined here with the sample in 100 mM KCl (3.54) is higher than that reported earlier for OMTKY3 in 10 mM KCl (3.2). This discrepancy can be attributed to a difference in salt concentration. As noted by Forsyth and Robertson (*23*), the pK_a of $P_{1'}$-Glu^{19} is sensitive to ionic strength. With no added salt, we obtained a pK_a value of 3.42 for this residue. The origin of the pK_a perturbation of $P_{1'}$-Glu^{19} has been attributed in part to the hydrogen bond between P_2-Thr^{17} $H^{\gamma1}$ and $P_{1'}$-Glu^{19} $O^{\epsilon1/\epsilon2}$ and in part to the intraresidue hydrogen bond between the backbone amide and side chain carboxylate of P_1'-Glu^{19} (*24*, *29*) as observed in X-ray structures of OMSVP3 (*30*) and the NMR structure of OMTKY3 (*31*). This interaction affects the dynamics of the side chain of $P_{1'}$-Glu^{19}, rendering signals from the $^1H^{\gamma2}$ and $^1H^{\gamma3}$ protons unobservable by [^{1}H,^{1}H]-TOCSY at neutral pH (when $P_{1'}$-Glu^{19} is deprotonated). A positive correlation was observed between the pH$_{mid}$ values of P_2-Thr^{17} and the pK_a values of $P_{1'}$-Glu^{19} in a large number of OMTKY3 variants (Figure 3). Systematic pK_a deviations were observed for other titratable residues at the $P_{1'}$ site; all were considerably lower than the standard pK_a values.

Effect of Disrupting the P_2-Thr^{17}···$P_{1'}$-Glu^{19} Hydrogen Bond. How will disruption of the hydrogen bond between P_2-Thr^{17} and $P_{1'}$-Glu^{19} affect the titration properties of the $P_{1'}$-Glu^{19} side chain? To answer this question, an OMTKY3 mutant was designed with P_2-Thr^{17} replaced with Val. [^{1}H,^{1}H]-TOCSY results for this variant (P_2-Thr^{17}Val) showed doubling of peaks indicative of two conformational states interconverting on a millisecond or longer time scale. Signals were assigned to individual residues, including $P_{1'}$-Glu^{19}, P_3-Cys^{16}, and P_4-Ala^{15} (Figure 4a). The relative volumes of the two sets of peaks were insensitive to pH; the mole fraction of the major form (I_a) was ~0.7, and the mole fraction of the minor form (I_b) was ~0.3 (Figure 4b) over the pH range that was investigated. Peaks were assigned to $P_{1'}$-Glu^{19} on the basis of peak pattern and chemical shift. The minor (I_T) $P_{1'}$-Glu^{19} spin system exhibited a pH-dependent $^1H^N$ chemical shift but no resolved $H^{\gamma2/\gamma3}$ peak at neutral pH, whereas the major (I_C) $P_{1'}$-Glu^{19} spin system exhibited a pH-independent $^1H^N$ chemical shift and a resolved, pH-dependent $H^{\gamma2/\gamma3}$ peak. The pK_a values for $P_{1'}$-Glu^{19} in the two conformational states, as determined from the pH dependence of these peaks, were both 3.92 (Table 3). Comparison of the results for wild-type and P_2-Thr^{17}Val OMTKY3 (Table 3) showed that disruption of the hydrogen bond between P_2-Thr^{17} and $P_{1'}$-Glu^{19} leads to elevation of the pK_a value of $P_{1'}$-Glu^{19} by 0.38 ± 0.05 pH unit. Disruption of this H-bond lowers the magnitude of the titration shift of $P_{1'}$-Glu^{19} $^1H^N$ by 0.43 ppm, showing that the intraresidue hydrogen bond between $^1H^N$ of $P_{1'}$-Glu^{19} and its carboxylate is weakened. The origin of the conformational heterogeneity in the P_2-Val^{17} variant remains unknown; however, one of its consequences is that the major form retains the hydrogen bond between $^1H^N$ of $P_{1'}$-Glu^{19} and its carboxylate, whereas the minor form does not.

Interactions among the P_2, $P_{1'}$, and $P_{3'}$ Sites (Residues 17, 19, and 21, Respectively). Figure 5 shows the local geometry of P_2-Thr^{17}, $P_{1'}$-Glu^{19}, and $P_{3'}$-Arg^{21} in the X-ray structure of the free silver pheasant ovomucoid third domain (*30*) (no X-ray structure is available for free OMTKY3, but that from the silver pheasant third domain, which has the same local sequence, should be a good approximation). The side chains of $P_{1'}$-Glu^{19} and $P_{3'}$-Arg^{21} are spatially proximate and have opposite charges; thus, an interaction between these two groups could contribute to the abnormally low pK_a of $P_{1'}$-

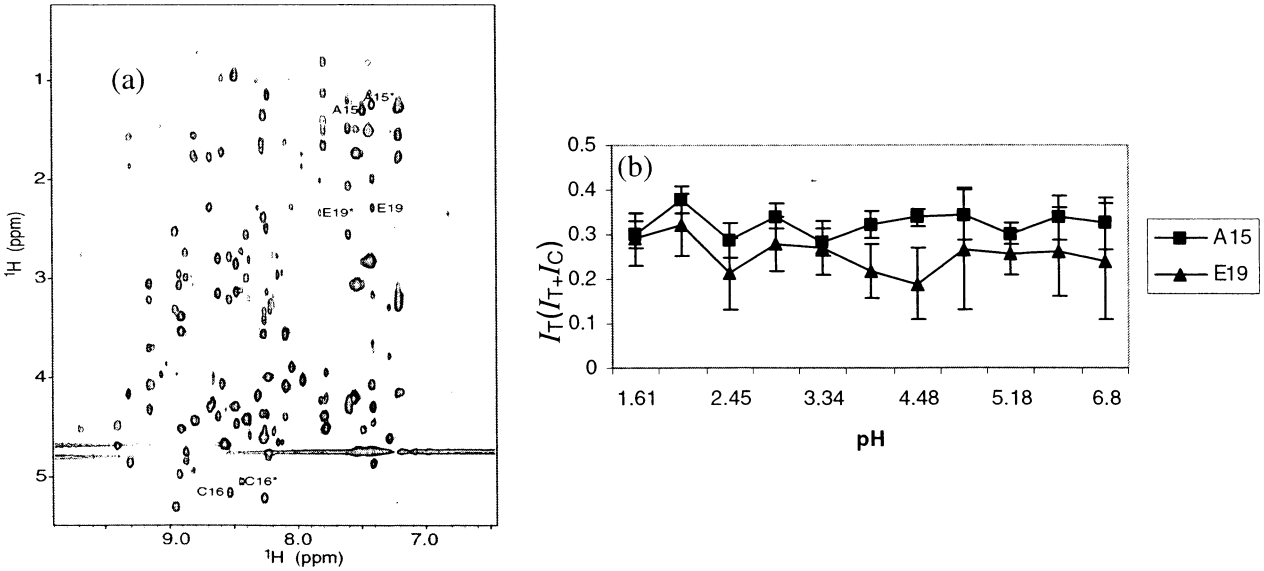

FIGURE 4: (a) Selected [^{1}H,^{1}H]-TOCSY region of P_2-Thr^{17}Val OMTKY3 at pH 4.1. For doubled resonances, that from the conformer with the trans P_8-Tyr^{11}−P_7-Pro^{12} peptide bond is denoted with an asterisk. (b) Population of the trans conformer as a function of pH as determined from the relative peak volumes [$I_T/(I_C + I_T)$] of doubled resonances from P_5-Ala^{15} and $P_{1'}$-Glu^{19}. Error estimates were derived from measurements of spectral noise.

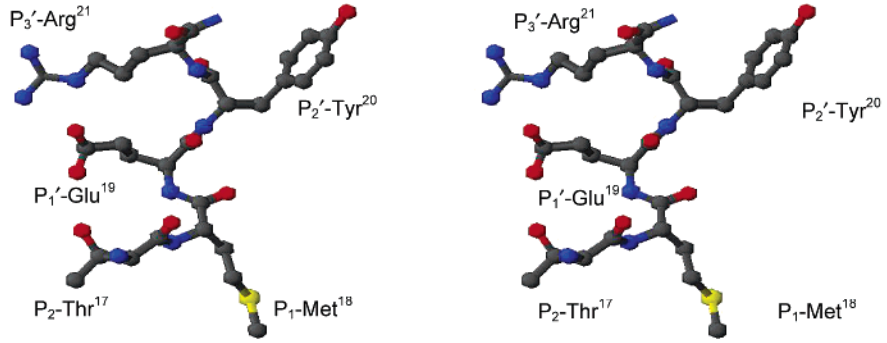

FIGURE 5: Stereoscopic representation of residues P_2-Thr^{17} to $P_{3'}$-Arg^{21} in the X-ray structure of the free silver pheasant ovomucoid third domain (*30*). These same residues (except P_1) are present in the turkey ovomucoid third domain, and thus, the structure should be similar. The color scheme is as follows: gray for carbon, blue for nitrogen, red for oxygen, and yellow for sulfur.

Glu^{19}. In fact, the current study provides evidence for such an effect. In most variants studied here that contained $P_{3'}$-Arg^{21} and Glu^{19} or Asp^{19} at $P_{1'}$, the chemical shift of $P_{3'}$-Arg^{21} $^1H^{\epsilon}$ was found to shift with increasing pH to a higher frequency by 0.06−0.07 ppm (see Table S1 of the Supporting Information). Although this titration shift is relatively small, the transition yields a measurable pH_{mid} value, which corresponds to the pK_a of the $P_{1'}$ side chain carboxylate.

As one example, Figure 6a shows the titration curve for $P_{3'}$-Arg^{21} $^1H^{\epsilon}$ (in P_2-Thr^{17}Val); the pH_{mid} of 3.71 derived from this curve is close to the pK_a determined for $P_{1'}$-Glu^{19} in this variant (3.92) (Figure 6b). As another example, the pK_a value of $P_{1'}$-Asp^{19} (in $P_{1'}$-Glu^{19}Asp OMTKY3) determined to be 3.13 from the pH dependence of its $^1H^{\beta2/\beta3}$ was equivalent within experimental error to the pH_{mid} for $P_{3'}$-Arg^{21} in the same molecule (determined to be 3.21 from the pH dependence of its $^1H^{\epsilon}$). $^1H^{\epsilon}$ of $P_{3'}$-Arg^{21} has a titration shift of 0.20 ppm for this transition (Table S1), consistent with a hydrogen bond between the two side chains.

Additional evidence for interactions among the P_2, $P_{1'}$, and $P_{3'}$ residues came from the titration curves of these residues in $P_{3'}$-Arg^{21}His OMTKY3. As shown in Figure 7, the $^1H^N$ chemical shifts of P_2-Thr^{17} and $P_{1'}$-Glu^{19} both exhibit a biphasic pH dependence. The higher pH_{mid} values were 6.07 (P_2-Thr^{17}) and 6.58 ($P_{1'}$-Glu^{19}) (see Table S2 of the Supporting Information); the latter is close to the pK_a (6.72) of $P_{3'}$-His^{21} (determined from the pH dependence of its $^1H^{\epsilon1}$). The lower pH_{mid} values were 3.44 (P_2-Thr^{17}) and 3.42 ($P_{1'}$-Glu^{19}) (Table S2); these are close to the lower pH_{mid} (3.28) determined from the biphasic pH dependence of $P_{3'}$-His^{21} $^1H^{\delta2}$ (Table S2). $^1H^N$ of $P_{1'}$-Glu^{19} shifts to a lower frequency upon deprotonation of $P_{3'}$-His^{21}; this suggests that the hydrogen bond between the backbone amide group and side chain carboxylate is disturbed by the neighboring imidazolium ion.

A similar effect was observed in $P_{3'}$-Arg^{21}Ala OMTKY3, in which replacement of Arg with Ala resulted in a change in the titration shift of $P_{1'}$-Glu^{19} $^1H^N$ of 0.14 ppm (Table 3). In this variant, the pK_a value determined for $P_{1'}$-Glu^{19} (3.77) was 0.23 ± 0.04 pH unit higher than in wild-type OMTKY3. These results suggest that the positive charge on $P_{3'}$-Arg^{21} makes a contribution of ~0.2 pH unit to the abnormally low pK_a of $P_{1'}$-Glu^{19} in wild-type OMTKY3.

As expected from electrostatics, the effect of placing a negative charge at $P_{3'}$ should be to elevate the pK_a of $P_{1'}$-Glu^{19}. This effect was observed (Table 3) in mutants $P_{3'}$-Arg^{21}Asp ($P_{1'}$-Glu^{19} pK_a = 3.91) and $P_{3'}$-Arg^{21}Glu ($P_{1'}$-Glu^{19} pK_a = 3.91). Most notably, the mutant $P_{3'}$-Arg^{21}Glu exhibited

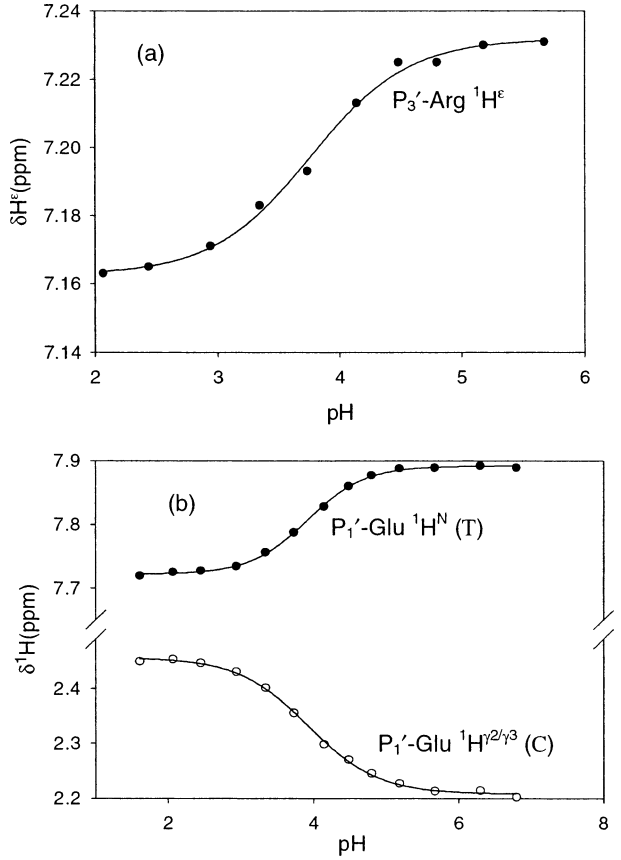

FIGURE 6: pH dependence of the chemical shifts of resonances in P_2-Thr^{17}Val OMTKY3: (a) $P_{3'}$-Arg side chain $^1H^{\epsilon}$, (b) $P_{1'}$-Glu backbone $^1H^N$ (T, signal from the minor conformational form observed with this mutant), and $P_{1'}$-Glu side chain $^1H^{\gamma 2/\gamma 3}$ (C, signal from the major conformational form observed with this mutant).

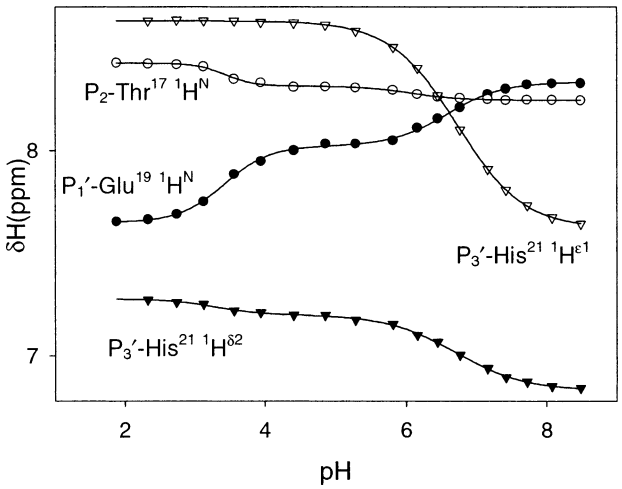

FIGURE 7: Chemical shifts of resonances from residues in $P_{3'}$-Arg^{21}His OMTKY3 plotted as a function of pH: P_2-Thr^{17} backbone $^1H^N$, $P_{1'}$-Glu^{19} backbone $^1H^N$, and $P_{3'}$-His^{21} ring $H^{\epsilon 1}$ and $^1H^{\delta 2}$.

increased titration shifts for $P_{1'}$-Glu^{19} $^1H^N$ (by 0.68 ppm) and P_2-Thr^{17} $^1H^N$ (by 0.15 ppm) (Table 3 and Table S3 of the Supporting Information); this indicates that the hydrogen bond between the side chains of P_2-Thr^{17} and $P_{1'}$-Glu^{19} and the intraresidue hydrogen bond of $P_{1'}$-Glu^{19} are much stronger in this variant than in wild-type OMTKY3.

In the mutant P_2-Thr^{17}Glu, $^1H^N$ of P_2-Glu^{17} exhibited a titration shift of 0.92 ppm and an associated pH_{mid} of 3.91 (Table 2). These results are consistent with the presence of a charged hydrogen bond between the backbone amide H^N and one or both O^{ϵ} atoms of P_2-Glu^{17} at neutral pH, which is disrupted when the side chain is protonated (with a pK_a of 3.91). As with $P_{1'}$-Glu^{19}, signals from P_2-Glu^{17} $^1H^{\gamma 2/\gamma 3}$ were not observed in the [^{1}H,^{1}H]-TOCSY data from samples at neutral pH, probably as the result of exchange broadening associated with the dynamics of the hydrogen-bonded system. In P_2-Thr^{17}Glu, the pK_a of $P_{1'}$-Glu^{19} was 3.87 as determined from the pH dependence of a $^1H^{\gamma 2/\gamma 3}$ signal; the pK_a increase in the mutant can be attributed to disruption of the hydrogen bond and to electrostatic interaction between negative charges at the $P_{1'}$ and P_2 sites.

A double mutant (P_2-Thr^{17}Val/$P_{3'}$-Arg^{21}Ala) OMTKY3 was constructed and investigated by NMR pH titration as a further test of interactions among the side chains at $P_{3'}$, $P_{1'}$, and P_2. The pK_a of $P_{1'}$-Glu^{19} in the double mutant derived from the pH dependence of its $^1H^{\gamma}$ signal (pH_{mid} = 4.10, Table 1) was 0.5−0.6 pH unit higher than that in wild-type OMTKY3, in agreement with the proposed network of interactions among $P_{1'}$-Glu^{19}, P_2-Thr^{17}, and $P_{3'}$-Arg^{21}. The lack of an observable titration shift for $^1H^N$ of $P_{1'}$-Glu^{19} in the double mutant suggests that the hydrogen bond between the side chain carboxyl group of $P_{1'}$-Glu^{19} and its backbone amide group is abolished in P_2-Thr^{17}Val/$P_{3'}$-Arg^{21}Ala.

Interactions between the Side Chain of $P_{1'}$ (Residue 19) and the Side Chains of P_1 and $P_{2'}$ (Residues 18 and 20). The introduction of negatively charged side chains at the neighboring $P_{2'}$ position had the effect of increasing the pK_a of $P_{1'}$-Glu^{19} by 0.32−0.44 pH unit (Table 3). The Hill coefficient for $P_{1'}$-Glu^{19} in $P_{2'}$-Tyr^{20}Asp was found to deviate slightly from unity. On the other hand, the conserved backbone conformation of the proteinase binding loop causes the side chains of P_1 and $P_{1'}$ to protrude in opposite directions (Figure 5). Electrostatic interactions between the side chains of these two residues appear to be minimal. The pK_a values of each of the four titratable residues (Asp, Glu, His, and Lys) inserted in the P_1 site were close to standard values. The pH dependence of $^1H^N$ of $P_{1'}$-Glu^{19} yielded a pH_{mid} of 3.21 in P_1-Leu^{18}Asp and a pH_{mid} of 3.39 in P_1-Leu^{18}Glu (Table 3).

Effect of Replacing P_1-Leu^{18} with Ala or Gly. The P_1 residue is the major determinant of binding specificity. OMTKY3, which has P_1-Leu, binds strongly to chymotrypsin. To extend studies of the linearity of substitutions at this key position to residues that permit additional flexibility, we examined pH titration effects in two additional variants: P_1-Leu^{18}Ala and P_1-Leu^{18}Gly. In P_1-Leu^{18}Ala, the pK_a value of $P_{1'}$-Glu^{19} (3.52 as determined from its $^1H^N$) and its titration shift (0.56 ppm) are comparable with those of wild-type OMTKY3. These results indicate that the backbone conformation of the P_1 and $P_{1'}$ sites is maintained in this mutant. In P_1-Leu^{18}Gly, signals from $P_{1'}$-Glu^{19} were well-resolved even at neutral pH. This permitted the determination of pH_{mid} values derived from the pH dependence of $P_{1'}$-Glu^{19} $^1H^{\gamma 2/\gamma 3}$ (3.32) and $^1H^N$ (3.47 with a 0.59 ppm titration shift).

$P_{2'}$ Replacements. Replacement of $P_{2'}$-Tyr of OMTKY3 with Asp or His has been found to increase the hydrolysis constant for cleavage of the reactive site peptide bond (K_{hyd}) by a factor of 5 (*29*). The titration data for these two mutants were compared with those for wild-type OMTKY3 for possible clues to the origin of this effect; however, nothing of significance was detected. In particular, there was no

evidence that these mutations decrease the strength of the hydrogen bond between $P_{1'}$-Glu and P_2-Thr. In $P_{2'}$-Tyr^{20}Asp, $^1H^N$ of P_2-Thr^{17} exhibits a pH_{mid} of 4.11 with a titration shift of −0.20 ppm. In $P_{2'}$-Tyr^{20}His, $^1H^N$ of P_2-Thr^{17} exhibits a pH_{mid} of 3.47 with a titration shift of −0.17 ppm. The magnitudes of these titration shifts are comparable to that in wild-type OMTKY3 (−0.24 ppm) (see Table S3 of the Supporting Information).

CONCLUSIONS

NMR pH titration investigations of OMTKY3 variants with titratable residues at all contact positions with proteinases have revealed a detailed picture of molecular interactions within this important part of the inhibitor.

Correlation of pK_a Values with Solvent Exposure. The pK_a values of titratable residues substituted into the P_5, P_4, and P_1 positions were found to be nearly identical to standard values from model compounds. An independent study of cyclodextrin binding has shown that P_4 and P_1 are the most solvent-exposed sites in the loop (*32*).

Perturbed pK_a Values at the P_2 and $P_{1'}$ Sites. The pK_a values of titratable side chains located at the P_2 and $P_{1'}$ sites show considerable deviation from standard pK_a values (Table 2). A consistent finding of this study is that residues at the $P_{1'}$ site have pK_a values consistently lower than normal. Although previous electrostatic calculations suggested that the amino group of $P_{16'}$-Lys^{34} makes the largest contribution to lowering the pK_a of $P_{1'}$-Glu^{19} (*23*), a later study by Forsyth and Robertson (*33*) showed that the carboxyl pK_a of $P_{1'}$-Glu^{19} is not elevated by replacement of $P_{16'}$-Lys^{34}. By combined pH titration and site-directed mutagenesis, the origin of the low pK_a of $P_{1'}$-Glu^{19} in OMTKY3 has been thoroughly probed in this study. Our results indicate that the major interactions responsible for lowering the pK_a of $P_{1'}$-Glu^{19} are the hydrogen bond between the carboxylate of $P_{1'}$-Glu^{19} and the hydroxyl group of P_2-Thr^{17}, the charge−charge interaction between $P_{1'}$-Glu^{19} and $P_{3'}$-Arg^{21}, and the intraresidue hydrogen bond between the carboxylate of $P_{1'}$-Glu^{19} and its own amide group. The hydrogen bond between $P_{1'}$-Glu^{19} and P_2-Thr^{17}, which is believed to help fix the conformation of the reactive site, lowers the pK_a of $P_{1'}$-Glu^{19} by ∼0.5 pH unit; disruption of this hydrogen bond increases the pK_a of $P_{1'}$-Glu^{19} from 3.54 to 3.92. On the other hand, the electrostatic effect of $P_{3'}$-Arg^{21} decreases the pK_a of $P_{1'}$-Glu^{19} by 0.2 pH unit. Interestingly, the effects of the two mutations affecting the pK_a of $P_{1'}$-Glu^{19} are additive: the pK_a shift of the double mutant (P_2-Thr^{17}Val/$P_{3'}$-Arg^{21}Ala) is equivalent to the sum of those of the two single mutants (Table 3).

As shown in the X-ray structure of OMSVP3 in its free form (*30*) (Figure 5), the distance between $P_{1'}$-Glu^{19} $O^{\epsilon 1/\epsilon 2}$ and P_2-Thr^{17} $O^{\gamma 1}$ is 3.0 Å, close enough for hydrogen bond formation. In addition, C^{ζ} of $P_{3'}$-Arg^{21} is 5.0 Å from the two O^{ϵ} atoms of $P_{1'}$-Glu^{19}, close enough for an important electrostatic interaction.

The electrostatic effects observed in this study are consistent with earlier observations by Robertson and coworkers (*24*), who found that the pK_a of $P_{1'}$-Glu^{19} is elevated at high salt. The results presented here demonstrate the interrelatedness of three interactions involving $P_{1'}$-Glu^{19}: the hydrogen bond between P_2-Thr^{17} $H^{\delta 1}$ and $P_{1'}$-Glu^{19} $O^{\epsilon 1/\epsilon 2}$, the electrostatic effect between the $P_{1'}$-Glu^{19} and $P_{3'}$-Arg^{21} side chains, and the intraresidue hydrogen bond between $P_{1'}$-Glu^{19} $O^{\epsilon 1/\epsilon 2}$ and H^N. This intraresidue hydrogen bond becomes weaker with the disruption of the hydrogen bond between P_2-Thr^{17} and $P_{1'}$-Glu^{19}.

Other Unusual pK_a Values. In addition to $P_{1'}$-Glu, other residues with obviously perturbed pK_a values in wild-type OMTKY3 include P_6-Lys^{13}, P_{12}-Asp^7, $P_{9'}$-Asp^{27}, $P_{16'}$-Lys^{34}, $P_{25'}$-Glu^{43}, $P_{34'}$-His^{52}, and C-terminal $P_{36'}$-Cys^{56} (*23*, *24*) (also, see Table S4 of the Supporting Information). The origins of most of these unusual pK_a values have been discussed in earlier studies (*23*, *24*, *33*). Nevertheless, the low pK_a values observed for P_6-Lys^{13} and $P_{16'}$-Lys^{34} and the high pK_a observed for $P_{25'}$-Glu^{43} remain puzzling. This study shows that the pK_a values of titratable residues in the core of OMTKY3 are not perturbed by replacements at positions in the proteinase binding loop (except for those at the $P_{3'}$ site).

Unusual pK_a values for many types of residues have been reported in previous studies (*2*−*5*, *27*, *34*−*36*). Perturbations of pK_a values result from various factors, such as charge−charge interactions between charged groups (*37*, *38*), the degree of solvent exposure of the charged group (*4*, *35*), hydrogen bond interaction (*9*), etc. For example, a pK_a of 6.36 for a glutamate side chain in rat CD2 has been attributed to mutual electrostatic repulsion (*37*). A pK_a of 7.5 for an aspartate side chain in oxidized *Escherichia coli* thioredoxin has been explained in terms of the hydrophobic local environment of the carboxyl group (*35*). In addition, the dipole associated with an α-helix can perturb the pK_a of a group located at the N- or C-terminus of the helix (*27*, *39*, *40*). In barnase, the pK_a values of histidyl residues located at the C-termini of α-helices were found to be ∼0.5 pH unit higher than normal, whereas those located at N-termini were 0.8 pH unit lower (*27*),

In OMTKY3, the side chains of P_8-Tyr^{11}, P_6-Lys^{13}, and $P_{16'}$-Lys^{34} are spatially close to one other, forming a cooperative triad. The local hydrophobic environment created by the side chains of these three residues may favor the neutral forms of P_6-Lys^{13}/Glu^{13}/Asp^{13} and $P_{16'}$-Lys^{34}; this would explain the perturbed pK_a values of these residues. The three-dimensional structure of OMTKY3 provides no evidence for hydrogen bond or charge−charge interactions responsible for the elevated pK_a of $P_{25'}$-Glu^{43}. However, the side chain of this residue is located at the C-terminus of the only α-helix in OMTKY3. As proposed by Hol et al. (*39*), the helix macrodipole is expected to place negative charge on the C-terminus and increase the pK_a of $P_{25'}$-Glu^{43}.

Origin of Chemical Shift Perturbations. Backbone $^1H^N$ resonances exhibiting significant titration shifts fall into two groups: those that shift with increasing pH to higher frequencies [$\Delta\delta(^1H^N) > 0$] and those that shift to lower frequencies [$\Delta\delta(^1H^N) < 0$]. As pointed out previously (*8*), a positive $\Delta\delta(^1H^N)$ is consistent with the formation of a (stronger) hydrogen bond between H^N and a newly formed carboxylate oxygen. An example of such an interaction is the amide group of $P_{1'}$-Glu^{19} of OMTKY3. The hydrogen bond between the side chain carboxylate and backbone amide is observed in X-ray and NMR structures of OMTKY3. In earlier studies of peptides, a negative $\Delta\delta(^1H^N)$ generally was interpreted as an "intrinsic titration" effect (*8*). However, our study shows that many such shifts are better explained by electrostatic shielding. For example, in the mutant P_4-

Ala[15]Asp, $^1H^N$ of P_4-Asp[15] yielded a $\Delta\delta(^1H^N)$ of −0.05 ppm, whereas its neighbor P_3-Cys[16] had a $\Delta\delta(^1H^N)$ of −0.14 ppm, with a pH_{mid} of 3.96, close to the pK_a value of P_4-Asp[15] (4.05). As another example, although no acidic residues are adjacent to $P_{15'}$-Asn[33], one of the $^1H^{\beta2/\beta3}$ signals of $P_{15'}$-Asn[33] shows a titration shift of −0.1 ppm with a pH_{mid} close to the pK_a of $P_{1'}$-Glu[19]. Since hydrogen bonds were observed only between the side chain amide group of $P_{15'}$-Asn[33] and the backbone oxygens of P_2-Thr[17] and $P_{1'}$-Glu[19], the titration shift of $P_{15'}$-Asn[33] $^1H^{\beta2/\beta3}$ most likely arises from an electrostatic effect from $P_{1'}$-Glu[19]. A similar phenomenon has been reported in rat CD2 (*37*), where the chemical shift of $H^{\gamma2/\gamma3}$ of Glu[29] was found to be influenced more strongly by a neighboring residue (Glu[41]) than by its intraresidue carboxyl group.

The magnitudes of most intrinsic titration effects on $^1H^N$ are on the order of approximately −0.05 ppm. In this study, however, many of the Asp and Glu residues with observable $^1H^N$ titration shifts to lower frequency had shifts in excess of 0.1 ppm. More work needs to be done in correlating titration shifts with structural information and pK_a values.

This study also shows that different protons on the same residue can yield different pH_{mid} values. A case in point is P_2-Asp[17] in the mutant P_2-Thr[17]Asp for which three distinct pH_{mid} values were determined from the pH dependence of its $^1H^N$, $^1H^{\beta2}$, and $^1H^{\beta3}$ protons (Figure 2 and Table 1). The protons of P_2-Asp[17] experience electrostatic effects from its own side chain and that of $P_{1'}$-Glu[19]. Special caution needs to be taken when determining pK_a values from the pH dependence of a single resonance in a complicated environment involving multiple charged groups. It can be difficult to distinguish intrinsic pK_a values from spectroscopic effects from neighboring titrating groups. Additional data may be needed to disentangle these factors such as the pH dependence of ^{13}C NMR signals from (selectively) ^{13}C-labeled protein.

ACKNOWLEDGMENT

We thank Dr. Zheng-Ping Yi for careful reading of the manuscript.

SUPPORTING INFORMATION AVAILABLE

Four tables of ^1H NMR chemical shifts, measured pH_{mid} values, measured pK_a values, and Hill coefficients of various residues. This material is available free of charge via the Internet at http://pubs.acs.org.

REFERENCES

1. Schechter, I., and Berger, A. (1967) *Biochem. Biophys. Res. Commun. 27*, 157−162.
2. Fersht, A. R. (1985) *Enzyme Structure and Mechanism*, W. H. Freeman and Co., New York.
3. Honig, B. H., Hubbell, W. L., and Flewelling, R. F. (1986) *Annu. Rev. Biophys. Biophys. Chem. 15*, 163−193.
4. Matthew, J. B., Gurd, F. R., Garcia-Moreno, B., Flanagan, M. A., March, K. L., and Shire, S. J. (1985) *CRC Crit. Rev. Biochem. 18*, 91−197.
5. Nakamura, H. (1996) *Q. Rev. Biophys. 29*, 1−90.
6. Bundi, A., and Wüthrich, K. (1979) *Biopolymers 18*, 285−297.
7. Russell, S. T., and Warshel, A. (1985) *J. Mol. Biol. 185*, 389−404.
8. Bundi, A., and Wüthrich, K. (1979) *Biopolymers 18*, 299−311.
9. Szyperski, T., Antuch, W., Schick, M., Betz, A., Stone, S. R., and Wüthrich, K. (1994) *Biochemistry 33*, 9303−9310.
10. Laskowski, M., Jr., and Kato, I. (1980) *Annu. Rev. Biochem. 49*, 593−626.
11. Bode, W., and Huber, R. (1992) *Eur. J. Biochem. 204*, 433−451.
12. Lu, S. M., Lu, W., Qasim, M. A., Anderson, S., Apostol, I., Ardelt, W., Bigler, T., Chiang, Y. W., Cook, J., James, M. N., Kato, I., Kelly, C., Kohr, W., Komiyama, T., Lin, T. Y., Ogawa, M., Otlewski, J., Park, S. J., Qasim, S., Ranjbar, M., Tashiro, M., Warne, N., Whatley, H., Wieczorek, A., Wieczorek, M., Wilusz, T., Wynn, R., Zhang, W., and Laskowski, M., Jr. (2001) *Proc. Natl. Acad. Sci. U.S.A. 98*, 1410−1415.
13. Qasim, M. A., Ranjbar, M. R., Wynn, R., Anderson, S., and Laskowski, M., Jr. (1995) *J. Biol. Chem. 270*, 27419−27422.
14. Qasim, M. A., Lu, S. M., Ding, J. H., Bateman, K. S., James, M. N. G., Anderson, S., Song, J. K., Markley, J. L., Ganz, P. J., Saunders, C. W., and Laskowski, M., Jr. (1999) *Biochemistry 38*, 7142−7150.
15. Choe, S. (1997) Studies of pH Effects on the Structure and Chemical Properties of Turkey Ovomucoid Third Domain, Ph.D. Thesis, University of Wisconsin−Madison, Madison, WI.
16. Lu, W. (1994) Energetics of the interactions of ovomucoid third domain variants with different serine proteinases, Ph.D. Thesis, Purdue University, West Lafayette, IN.
17. Lu, W., Apostol, I., Qasim, M. A., Warne, N., Wynn, R., Zhang, W. L., Anderson, S., Chiang, Y. W., Ogin, E., Rothberg, I., Ryan, K., and Laskowski, M., Jr. (1997) *J. Mol. Biol. 266*, 441−461.
18. Hinck, A. P., Walkenhorst, W. F., Westler, W. M., Choe, S., and Markley, J. L. (1993) *Protein Eng. 6*, 221−227.
19. Assadi-Porter, F. M., Aceti, D. J., and Markley, J. L. (2000) *Arch. Biochem. Biophys. 376*, 259−265.
20. Bates, R. G. (1973) Determination of pH: theory and practice, pp 59−104, John Wiley and Sons, New York.
21. Sklenár, V., Piotto, M., Leppik, R., and Saudek, V. (1993) *J. Magn. Reson., Ser. A 102*, 241−245.
22. Markley, J. L. (1975) *Acc. Chem. Res. 8*, 70−80.
23. Forsyth, W. R., Gilson, M. K., Antosiewicz, J., Jaren, O. R., and Robertson, A. D. (1998) *Biochemistry 37*, 8643−8652.
24. Schaller, W., and Robertson, A. D. (1995) *Biochemistry 34*, 4714−4723.
25. Robertson, A. D., Westler, W. M., and Markley, J. L. (1988) *Biochemistry 27*, 2519−2529.
26. Lehninger, A., Nelson, D., and Cox, M. (1992) *Principles of Biochemistry*, Worth Publishers, New York.
27. Sancho, J., Serrano, L., and Fersht, A. R. (1992) *Biochemistry 31*, 2253−2258.
28. Tanford, C. (1962) *Adv. Protein Chem. 17*, 69−165.
29. Ardelt, W., and Laskowski, M., Jr. (1991) *J. Mol. Biol. 220*, 1041−1053.
30. Bode, W., Epp, O., Huber, R., Laskowski, M., Jr., and Ardelt, W. (1985) *Eur. J. Biochem. 147*, 387−395.
31. Krezel, A. M., Darba, P., Robertson, A. D., Fejzo, J., Macura, S., and Markley, J. L. (1994) *J. Mol. Biol. 242*, 203−214.
32. Yi, Z.-P., Warrington, T. L., Qasim, M. A., Qasim, S., and Laskowski, M., Jr. (2001) *Protein Sci. 10*, 179.
33. Forsyth, W. R., and Robertson, A. D. (2000) *Biochemistry 39*, 8067−8072.
34. Andersen, J. F., Sanders, D. A., Gasdaska, J. R., Weichsel, A., Powis, G., and Montfort, W. R. (1997) *Biochemistry 36*, 13979−13988.
35. Langsetmo, K., Fuchs, J. A., and Woodward, C. (1991) *Biochemistry 30*, 7603−7609.
36. Yu, L., and Fesik, S. W. (1994) *Biochim. Biophys. Acta 1209*, 24−32.
37. Chen, H. A., Pfuhl, M., McAlister, M. S., and Driscoll, P. C. (2000) *Biochemistry 39*, 6814−6824.
38. Honig, B., and Nicholls, A. (1995) *Science 268*, 1144−1149.
39. Hol, W. G., van Duijnen, P. T., and Berendsen, H. J. (1978) *Nature 273*, 443−446.
40. Joshi, H. V., and Meier, M. S. (1996) *J. Am. Chem. Soc. 118*, 12038−12044.
41. Laskowski, M., Jr., Kato, I., Ardelt, W., Cook, J., Denton, A., Empie, M. W., Kohr, W. J., Park, S. J., Parks, K., and Schatzley, B. L. (1987) *Biochemistry 26*, 202−221.
42. Apostol, I., Giletto, A., Komiyama, T., Zhang, W., and Laskowski, M., Jr. (1993) *J. Protein Chem. 12*, 419−433.

BI0269512